Self-trapping of light in a two-dimensional photonic lattice

Ziad H. Musslimani

Department of Mathematics, University of Central Florida, Orlando, Florida 32816

Jianke Yang

Department of Mathematics and Statistics, University of Vermont, Burlington, Vermont 05401

Received July 21, 2003; revised manuscript received December 3, 2003; accepted December 15, 2003

We study wave propagation in a two-dimensional photonic lattice with focusing Kerr nonlinearity, and report on the existence of various nonlinear localized structures in the form of fundamental, dipole, and vortex solitons. First, the linear bandgap structure induced by the two-dimensional photonic crystal is determined, and solitons are found to exist in the photonic bandgap. Next, structures of these solitons and their stability properties are analyzed in detail. When the propagation constant is not close to the edge of the bandgap, the fundamental soliton is largely confined to one lattice site; the dipole soliton consists of two π-out-of-phase, Gaussian-like humps, whereas the vortex comprises four fundamental modes superimposed in a square configuration with a phase structure that is topologically equivalent to the conventional homogeneous-bulk vortex. At high lattice potential, all these soliton states are stable against small perturbations. However, among the three states, the fundamental solitons are the most robust, whereas vortices are the least. If the propagation constant is close to the edge of the bandgap, then all three soliton states spread over many lattice sites and become linearly unstable as a result of the Vakhitov–Kolokolov instability.

OCIS codes: 190.0190, 190.5530.

1. INTRODUCTION

Optical wave propagation in nonlinear periodic media, such as an array of optical waveguides, displays unique phenomena that are absent in homogeneous media. This is demonstrated most clearly by the existence of allowed bands and forbidden gaps in the linear spectrum. In these periodic structures, wave dynamics is governed by the interplay between optical tunneling to adjacent sites (or waveguides) and nonlinearity. A balance between these two effects could result in self-localized structures known as lattice solitons.[1]

In general, lattice solitons are localized modes of nonlinear waveguide arrays that form when discrete diffraction is counteracted by self-focusing nonlinearity.[2] They were first predicted theoretically in an optical waveguide array[3,4] as solutions of the discrete nonlinear Schrödinger equation. Later on, self-trapping of light in discrete nonlinear waveguide arrays was experimentally observed.[5,6] When a low-intensity beam is focused into a waveguide array, the propagating field spreads over many sites (as a result of optical tunneling), exhibiting a typical discrete diffraction pattern with the intensity concentrated mainly in the outer lobes. However, at sufficiently high power, the beam self-traps to form a localized state (a soliton) in the center waveguides. Subsequently, many interesting properties of wave propagation in one-dimensional (1D) lattices were reported. For example, linear and nonlinear Bloch oscillations in an array of AlGaAs,[7] polymer,[8] and curved optical waveguides[9] were experimentally observed.

Very recently, lattice solitons in 1D and two-dimensional (2D) photorefractive optical crystals were reported.[10–12] The experiments in Refs. 10–12 are particularly interesting since the 2D waveguide array is formed optically; thus, it is very versatile and easily tunable. This in turn allowed a host of 2D localization phenomena to be observed. Stimulated by these experiments, we have recently studied fundamental and vortex solitons in a 2D optical lattice with focusing Kerr nonlinearity,[13] and found that in the strong localization regime, fundamental solitons are stable against small perturbations. On the other hand, for a shallow lattice potential, vortex solitons were shown to be unstable. However, many questions concerning the stability and structure of localized modes remain open. For instance, what is the bandgap structure of linear waves propagating in a 2D lattice? How does the lattice potential depth affect the stability properties of fundamental and vortex solitons? How robust are these solitons against strong perturbations? Do other types of localized structures with different geometries exist as well?

In this paper, we comprehensively investigate beam propagation in a 2D photonic lattice in the presence of focusing Kerr nonlinearity. We first determine the bandgap structure for linear-wave propagation. This bandgap turns out to be identical to that in Mathieu's equation, and localized states can exist only inside the bandgap. Next, we study various nonlinear localized structures such as fundamental, dipole, and vortex solitons and analyze their stabilities. We identify two important localization limits on which the structure and stability properties of these solitons crucially depend. In the strong-

localization regime the propagation constant is not close to the edge of the bandgap. In this case, the fundamental soliton is confined largely on one lattice site with a uniform phase. A dipole soliton consists of two π-out-of-phase, Gaussian-like humps. The vortex soliton, on the other hand, comprises four fundamental modes located at the bottoms of the optical potential in a square configuration with a phase structure that is topologically equivalent to the conventional homogeneous-bulk vortex. By winding around the zero intensity position along any simple closed curve, the phase of the vortex state acquires 2π increments. In this regime, we show that the fundamental solitons are stable, while dipole and vortex solitons are stable only when the potential strength is sufficiently high. Increasing the potential strength has a stabilizing effect on these solitons. We have also tested the robustness of all three localized states, and found that fundamental solitons are the most robust against strong perturbations while vortex solitons are the least robust.

In the other localization limit the propagation constant is close to the bandgap. In this weak localization regime, all three types of soliton states spread over many lattice sites and are linearly unstable as a result of the Vakhitov–Kolokolov (VK) instability.

The paper is organized as follows. In Section 2 we present the model that describes the interaction between laser beam and periodic optical potential. Then we discuss in Section 3 the linear properties of wave propagation in periodic media and analyze the band structure. Nonlinear fundamental solitons are reported in Section 4, and their linear and nonlinear stability properties (including the question of collapse arrest) are subsequently discussed. In Sections 5 and 6 dipole and vortex solitons in the 2D lattice potential are described, and their stability properties determined. We conclude in Section 7.

2. MODEL

The equation that governs the evolution of a laser beam propagating in a self-focusing, nonlinear, inhomogeneous Kerr medium is given by

$$i\frac{\partial U}{\partial z} + \left(\frac{\partial^2}{\partial X^2} + \frac{\partial^2}{\partial Y^2}\right)U - \mathcal{V}U + |U|^2U = 0, \quad (1)$$

where U is the slowly varying envelope of the optical field propagating along the z direction. Here, the transverse X, Y coordinates are measured in units of the lattice spacing D and the propagation distance z in units of k_1D^2, where $k_1 = 2\pi n/\lambda_0$, λ_0 is the wavelength of the carrier field, and n is the refractive index of the material. Typical values for D vary between 6 and 20 μm, depending on whether we use AlGaAs or photorefractive crystals. In the above equation, $\mathcal{V}$ represents the optically induced photonic lattice which serves as an inhomogeneous environment for the propagating beam. Such optical crystals can be experimentally created by interfering pairs of laser beams polarized in such a way that the resulting beam will not "feel" the nonlinearity and will keep its linear standing wave pattern.[12,14] If we assume that both plane waves forming the lattice are mutually incoherent, the potential $\mathcal{V}$ takes the form

$$\mathcal{V} = \mathcal{V}_0(\cos^2 X + \cos^2 Y). \quad (2)$$

Here, we consider the focusing Kerr nonlinearity, which is different from the saturable nonlinearity used in recent experiments on 2D photorefractive lattice solitons.[10–12] However, our results have obvious implications to the saturable case, as structures of all three types of solitons are expected to be the same. Moreover, our findings can be directly applied as well to Bose–Einstein condensation in 2D optical lattices.

We next make an important comment regarding the sign of the lattice potential $\mathcal{V}_0$. In optical problems, $\mathcal{V}_0$ is generally negative. However, one can use a transformation $X \to X + \pi/2$, $Y \to Y + \pi/2$, and $\psi \to \psi\exp(-2i\mathcal{V}_0 z)$ to convert the $\mathcal{V}_0 < 0$ case to the $\mathcal{V}_0 > 0$ case. Thus we will assume $\mathcal{V}_0 > 0$ in this paper without any loss of generality.

Equation (1) conserves two quantities: the power

$$P = \int_{-\infty}^{\infty}\int_{-\infty}^{\infty}|U|^2 \mathrm{d}X\mathrm{d}Y, \quad (3)$$

and the energy E:

$$E = \int_{-\infty}^{\infty}\int_{-\infty}^{\infty}\left(|\nabla\psi|^2 - \frac{1}{2}|U|^4 + \mathcal{V}|U|^2\right)\mathrm{d}X\mathrm{d}Y. \quad (4)$$

These conserved quantities play an important role in determining the stability properties of localized modes.

We look for stationary solutions of the form

$$U(X, Y, z) = \exp(-i\mu z)u(X, Y), \quad (5)$$

where μ is the propagation constant of the soliton. Then $u(X, Y)$ satisfies

$$\frac{\partial^2 u}{\partial X^2} + \frac{\partial^2 u}{\partial Y^2} - \mathcal{V}u + |u|^2u = -\mu u. \quad (6)$$

Without the lattice potential, solitons would suffer collapse under small perturbations.[15,16] However, as we shall show here, optical lattices can suppress the collapse of solitons.

3. LINEAR SPECTRUM AND BANDGAP

To understand the mechanism behind energy localization, we consider first wave propagation in *linear* inhomogeneous media. Substituting Eq. (2) into Eq. (6) and neglecting the nonlinear term, we get

$$\left(\frac{\partial^2}{\partial X^2} + \frac{\partial^2}{\partial Y^2}\right)u - \mathcal{V}_0(\cos^2 X + \cos^2 Y)u = -\mu u. \quad (7)$$

The optical potential $\mathcal{V}(X, Y)$ is separable, which enables us to reduce the dimensionality of the problem and facilitate the understanding of the band structure. Indeed, by setting

$$u(X, Y) = u_1(X)u_2(Y), \quad (8)$$

we can split Eq. (7) into two 1D equations

$$\frac{\partial^2 u_1(X)}{\partial X^2} - \mathcal{V}_0\cos^2 X u_1(X) = -\mu_1 u_1(X), \quad (9)$$

$$\frac{\partial^2 u_2(Y)}{\partial Y^2} - \mathcal{V}_0\cos^2 Y u_2(Y) = -\mu_2 u_2(Y), \quad (10)$$

with

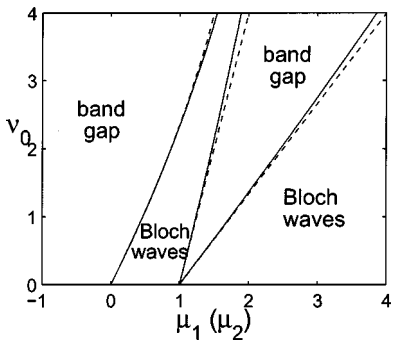

Fig. 1. Bandgap structure of the linear periodic problem of Eqs. (9) and (10). Solid curves, the numerically computed bandgap boundaries; dashed curves, analytic approximations of Eqs. (14)–(16) for the same boundaries.

$$\mu = \mu_1 + \mu_2. \tag{11}$$

Equations (9) and (10) are 1D Mathieu's equations whose properties are well known. According to the Bloch theorem, the eigenfunctions are given by

$$u_1(X) = \phi_k(X)\exp(ikX), \tag{12}$$

where k is the wave vector and $\phi_k(X) = \phi_k(X + \pi)$ is a π-periodic Bloch function. Due to periodicity, there is a gap in the linear spectrum, so wave localization can occur only for wave numbers k lying inside the gap. Otherwise, the system will be in a periodic extended state (Bloch state) and nonlinearity cannot cause the wave function to localize. In light of this fact, it is important to locate the boundaries of the gap to identify nonlinear localized waves. For this purpose, we write Eq. (9) as

$$\frac{\partial^2 u_1(X)}{\partial X^2} - \frac{\mathcal{V}_0}{2}[1 + \cos(2X)]u_1(X) = -\mu_1 u_1(X). \tag{13}$$

The bandgap structure of this Mathieu's equation is well known. Using the numerical algorithm described in Ref. 17, we have determined the boundaries of these band gaps. The boundaries for the first two bandgaps are shown in Fig. 1 (solid curves).

Using perturbation theories at small $\mathcal{V}_0$ values, one can obtain the leading-order approximations to the three boundary curves shown in Fig. 1 (from left to right) as[17]

$$\mu_1 \approx 1/2\mathcal{V}_0 - 1/32\mathcal{V}_0^2, \tag{14}$$

$$\mu_1 \approx 1 + 1/4\mathcal{V}_0, \tag{15}$$

and

$$\mu_1 \approx 1 + 3/4\mathcal{V}_0. \tag{16}$$

These approximations are also shown in Fig. 1 as dashed curves. We see that approximation (14) for the left-hand boundary curve is very good even for moderate values of $\mathcal{V}_0$, while approximations (15) and (16) for the right-hand two curves are not as good, especially when $\mathcal{V}_0$ is not small.

In this paper, we consider only gap solitons for which both μ_1 and μ_2 fall in the left-hand (first) bandgap in Fig. 1. In terms of $\mu = \mu_1 + \mu_2$, this bandgap is given by $-\infty < \mu < \mu_{\max}$, where $\mu_{\max} = 2\mu_{1,\max}$ and $\mu_{1,\max}(\mathcal{V}_0)$ is the left-hand curve in Fig. 1. This semi-infinite gap is the counterpart of $-\infty < \mu < 0$ in the lattice-free case ($\mathcal{V}_0 = 0$). For small or moderate values of $\mathcal{V}_0$, we see from Eq. (14) that $\mu_{\max}$ is well approximated by the function

$$\mu_{\max} = 2\mu_{1,\max} \approx \mathcal{V}_0 - \mathcal{V}_0^2/16. \tag{17}$$

Localized solutions to Eq. (6) must lie inside a bandgap, which is the semi-infinite region $-\infty < \mu < \mu_{\max}$ as far as this paper is concerned. Solitons in higher bandgaps will not be considered (such solitons in a 1D optical lattice have been studied in Refs. 18 and 19). With this in mind, we next proceed to identify various nonlinear localized structures. We emphasize, however, that even though the above bandgap structure was derived for the separable potential of Eq. (2), it should hold qualitatively for nonseparable potentials as well.

4. FUNDAMENTAL LATTICE SOLITONS AND THEIR STABILITY

A. Numerical Algorithm

Solutions to Eq. (6) in the form of fundamental, dipole, or vortex solitons can be obtained by a Fourier-iteration method. First we define the 2D Fourier transform:

$$\mathcal{F}(f) = \hat{f}(\mathbf{k}) = \int d\mathbf{x} f(\mathbf{x})\exp(-i\mathbf{k}\cdot\mathbf{x}), \tag{18}$$

with the inverse given by

$$f(\mathbf{x}) = \mathcal{F}^{-1}(\hat{f}) = \frac{1}{2\pi}\int d\mathbf{k}\hat{f}(\mathbf{k})\exp(+i\mathbf{k}\cdot\mathbf{x}). \tag{19}$$

By applying the Fourier transform to Eq. (6) we obtain

$$\hat{u} = -\frac{1}{|\mathbf{k}|^2 - \mu}\mathcal{F}(\mathcal{V}u) + \frac{1}{|\mathbf{k}|^2 - \mu}\mathcal{F}(|u|^2 u). \tag{20}$$

This is a fixed-point equation for $\hat{u}$ that can be solved by a homogenization method, as was suggested by Petviashvili.[20] However, note that Eq. (20) is singular on the circle defined by $|\mathbf{k}|^2 = \mu$ (when $\mu > 0$). To overcome this difficulty, we first add and subtract a term cu from Eq. (6), then take the Fourier transform. Here c is some positive constant. By doing so we arrive at the following iteration scheme:

$$\hat{u}_{m+1} = \frac{1}{c + |\mathbf{k}|^2}\left[\frac{\mathcal{P}(\eta_L)}{\mathcal{P}(\eta_N)}\right]^{1/2}[(\mu + c)\hat{u}_m - \mathcal{F}(\mathcal{V}u_m)] + \frac{1}{c + |\mathbf{k}|^2}\left[\frac{\mathcal{P}(\eta_L)}{\mathcal{P}(\eta_N)}\right]^{3/2}\mathcal{F}(|u_m|^2 u_m), \tag{21}$$

where we have defined the projection operator $\mathcal{P}$ by

$$\mathcal{P}(\hat{\phi}) \equiv \int d\mathbf{k}\hat{u}(\mathbf{k})\hat{\phi}(\mathbf{k}), \tag{22}$$

and

$$\eta_L = (|\mathbf{k}|^2 - \mu)\hat{u} + \mathcal{F}(\mathcal{V}u), \tag{23}$$

$$\eta_N = \mathcal{F}(|u|^2 u). \tag{24}$$

By choosing a Gaussian-like initial condition one can iterate the above Eq. (21) to obtain fundamental solitons.

These solitons have a single main hump sitting at a bottom of the potential, say $(X, Y) = (\pi/2, \pi/2)$. Two examples corresponding to propagation constants $\mu = 1$ and $\mu = 1.72$ with $\mathcal{V}_0 = 2$ are displayed in Fig. 2. These solitons have uniform phase but varying intensity distributions. At this potential strength, the left-hand bandgap in Fig. 1 is $-\infty < \mu < \mu_{\max} = 1.7563$, while numerically we have found that the fundamental solitons exist for $-\infty < \mu \lesssim 1.75$. The agreement is excellent. Thus we conclude that fundamental solitons exist in the entire left-hand bandgap of Fig. 1. When $\mu = 1$, which is not close to the band edge $\mu_{\max}$, the soliton is largely confined on one lattice site [see Fig. 2(a)], while at $\mu = 1.72$, which is very close to the band edge, it spreads over many lattice sites [see Fig. 2(b)]. This is not surprising, since as μ reaches this band edge, the u solution approaches the extended Bloch state and becomes periodic in both X and Y directions.

B. Power and Stability Analysis

To quantify these solitons, we calculate the dependence of the normalized power P on the propagation constant μ. When $\mathcal{V}_0 = 2$, the power curve is displayed in Fig. 3(a). We can see that as $\mu \to -\infty$, P approaches a constant value of 11.70. This is apparently because, in this limit, the fundamental soliton is highly localized; thus it approaches the lattice-free, fundamental-soliton state, which has power $P \approx 11.70$. As μ goes to the band edge at $\mu_{\max} = 1.7563$, the fundamental state becomes periodic in space; hence, P goes to infinity. At $\mu \approx 1.61$ which is quite close to the band edge, P has the minimal value of 4.49. At this point, $dP/d\mu$ changes sign; hence, the VK theorem suggests that the fundamental soliton changes its linear stability here. Specifically, when $\mu > 1.61$ where $dP/d\mu > 0$, the soliton should be linearly unstable with a purely real, unstable eigenvalue σ.[21] We have confirmed this instability by numerically simulating the linearized version of Eq. (1) around the fundamental soliton. By denoting $U = \exp(-i\mu z)[u(X, Y) + \tilde{U}(X, Y, z)]$, where $u(X, Y)$ is the fundamental soliton and $\tilde{U} \ll 1$ is the infinitesimal perturbation, the linearized equation for $\tilde{U}$ is

$$i\frac{\partial \tilde{U}}{\partial z} + \frac{\partial^2 \tilde{U}}{\partial X^2} + \frac{\partial^2 \tilde{U}}{\partial Y^2} + (\mu - \mathcal{V} + 2|u|^2)\tilde{U} + u^2\tilde{U}^* = 0. \tag{25}$$

Starting from a white-noise initial condition, we simulated Eq. (25) for a long distance (hundreds of z units). As expected, when $\mu > 1.61$, the solution of this linearized equation grows exponentially. The growth rate is the unstable eigenvalue σ, which we have obtained numerically and shown in Fig. 3(b), versus the propagation constant μ. When $\mu < 1.61\,(\mathcal{V}_0 = 2)$, the VK instability is absent. In this case, we have found numerically that linearized Eq. (25) has no exponentially growing modes; thus the soliton state is linearly stable.

When the fundamental soliton is linearly stable (i.e., no VK instability), it also happens to be nonlinearly stable.[13,22] Under small perturbations, the amplitude of the soliton oscillates slightly, and no collapse or breakup was observed. If the fundamental soliton suffers the VK instability, then under small perturbations, the soliton could evolve into a breathing state, or decay into radiation, depending on what perturbation is imposed.[13] This instability development is similar to that in a generalized nonlinear Schrödinger equation under VK instability.[23]

Next, we study the effect of potential strength $\mathcal{V}_0$ on fundamental solitons and their stability behavior. For this purpose, we have repeated the above calculations with a lower potential value $\mathcal{V}_0 = 1$, and the results are shown in Fig. 3 as well. At this potential value, the left-hand bandgap in Fig. 1 is $-\infty < \mu < 0.9379$, which is a little shorter than the bandgap at $\mathcal{V}_0 = 2$. Numerically, we have found fundamental solitons everywhere in this bandgap, and their powers are displayed in Fig. 3(a). We see that at this lower potential, the power needed to sustain the fundamental soliton is higher. In fact, the minimal power for $\mathcal{V}_0 = 1$ is now 7.11, which is much higher than the minimal power 4.49 at $\mathcal{V}_0 = 2$. Thus, we conclude that higher potential reduces the power required for generating fundamental solitons. The VK instability is not affected much by the potential strength, though. At $\mathcal{V}_0 = 1$, the VK instability occurs at $\mu \approx 0.72$ where the soliton power is minimal; the VK growth rate is plotted in Fig. 3(b) for comparison. We see that the growth curve at $\mathcal{V}_0 = 1$ is roughly the same as that at $\mathcal{V}_0 = 2$, except for a shift in location because the bandgap has been shifted. Thus, we conclude that higher potential does not significantly affect the linear stability properties of fundamental solitons. However, higher potential does improve the nonlinear stability behaviors of fundamental solitons (see below).

We have shown in Ref. 13 that linearly stable fundamental solitons in a 2D lattice do not collapse or break up under weak perturbations. Then how robust are linearly

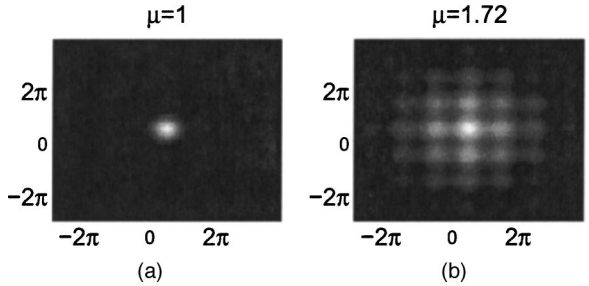

Fig. 2. Profiles of fundamental solitons at (a) $\mu = 1$ and (b) $\mu = 1.72$ with $\nu_0 = 2$.

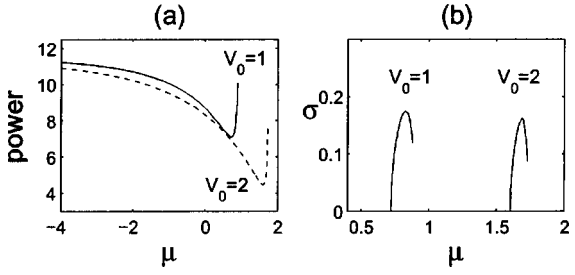

Fig. 3. (a) Normalized power P of fundamental solitons versus μ for $\nu_0 = 1$ and $\nu_0 = 2$; (b) unstable eigenvalues σ of these solitons.

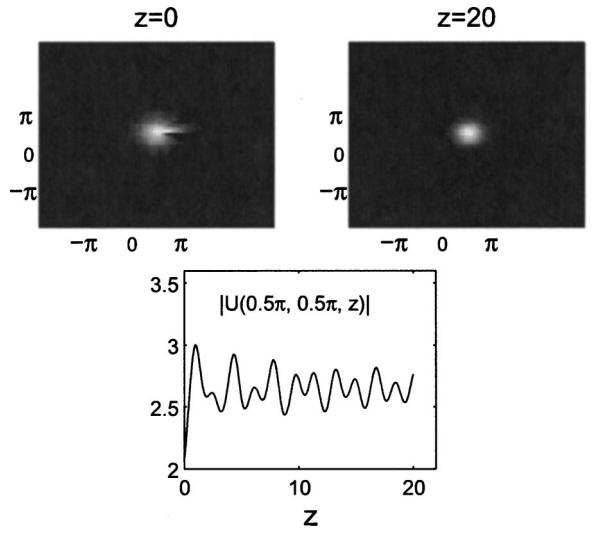

Fig. 4. Stable evolution of the fundamental soliton with $\mu = 1$ and $\nu_0 = 2$ under strong perturbations $\epsilon = 0.2$ in Eq. (26).

stable fundamental solitons under strong perturbations? To address this issue, we numerically study the nonlinear evolution of linearly stable fundamental solitons under the following "random noise" perturbations:

$$U(X, Y, z = 0) = u(X, Y)\left(1 + \epsilon + \epsilon \tanh \hat{r} \sum_{j=1}^{10} \sin j\hat{\theta}\right). \quad (26)$$

Here, $u(X, Y)$ is a fundamental soliton solution, $\hat{r}$ and $\hat{\theta}$ are the distance and angle of the point (X, Y) relative to the fundamental-state center $(\pi/2, \pi/2)$, and ϵ is the amplitude of perturbations. A number of simulations with various $\mathcal{V}_0$, μ, and ϵ values have been performed. We have found that linearly stable fundamental solitons are quite robust. For the purpose of illustration we select $\mathcal{V}_0 = 2$, $\mu = 1$, and $\epsilon = 0.2$. Evolution of the fundamental soliton under this perturbation is shown in Fig. 4. We see that the soliton can resist this strong perturbation and remain stable. In fact, we have found that for even larger values of ϵ, this perturbed soliton still remains stable. When the potential becomes weaker, obviously the soliton will become less robust. Indeed, at zero potential strength (i.e., the lattice-free case), the fundamental soliton can easily collapse even under very small perturbations.[15,16] Thus, higher potential does improve the nonlinear stability of fundamental solitons.

5. DIPOLE LATTICE SOLITONS AND THEIR STABILITY

Vector dipole solitons in a saturable nonlinear medium have been experimentally observed[24,25] and theoretically analyzed.[25,26] These composite solitons consist of two fields, a fundamental mode and a dipole mode, mutually trapped in their jointly induced potential well. Alternatively, one can view the fundamental mode as a waveguide that guides a dipole mode. In the present case, the lattice potential serves as a guiding component, and it can also guide (or trap) dipole modes. But major differences exist between dipole solitons in these two different physical situations. For instance, vector dipole solitons were shown to be always linearly stable,[25,26] while dipoles in a 2D lattice can be linearly unstable (see below). In this section, we study dipole lattice solitons and their stability properties.

Dipole-soliton solutions of Eq. (6) can be determined by the same iteration procedure as described in Section 4, by starting with an initial guess in the form of two π-out-of-phase Gaussian humps located at two diagonal potential wells such as $(-\pi/2, -\pi/2)$ and $(\pi/2, \pi/2)$. Two examples with $\mu = 1$ and $\mu = 1.70$ at $\mathcal{V}_0 = 2$ are displayed in Fig. 5. These solitons have zero phase in the upper diagonal half-plane $Y > -X$, and π phase in the lower diagonal half-plane $Y < -X$. At potential strength $\mathcal{V}_0 = 2$, we found numerically that these solitons exist in the propagation-constant interval $-\infty < \mu < \mu_{\text{dipole}} \approx 1.72$. Note that this upper bound μ_{dipole} is below the linear bandgap edge $\mu_{\max} = 1.7563$ of Fig. 1, not coinciding with it. This may be because the bandgap of Fig. 1 was derived for eigenfunctions of the separable type of Eq. (8), while the continuous-wave limit of dipole solitons as μ approaches the upper bound μ_{dipole} is not of that type. Indeed, all dipole solitons in this paper have zero intensity on the diagonal line $Y = -X$, hence these solitons cannot be of the separable type of Eq. (8) under continuous-wave limits. When μ is not close to the upper bound μ_{dipole}, the dipole soliton is more localized and consists of two Gaussian-like humps with π phase difference (see top row of Fig. 5). However, when μ is close to the upper bound μ_{dipole}, the soliton spreads out to more lattice sites (see bottom row of Fig. 5).

The power diagram of dipole solitons is similar to that of fundamental solitons, but is about twice higher. This can be seen in Fig. 6(a), where the power of dipole solitons is plotted against the propagation constant μ for two different potential values $\mathcal{V}_0 = 1$ and 2. By comparing Fig. 6(a) with Fig. 3(a), we see that dipole solitons' powers are roughly twice that of the fundamental solitons for the same value of μ. The reason is obviously that a dipole soliton can be thought of roughly as comprising two fun-

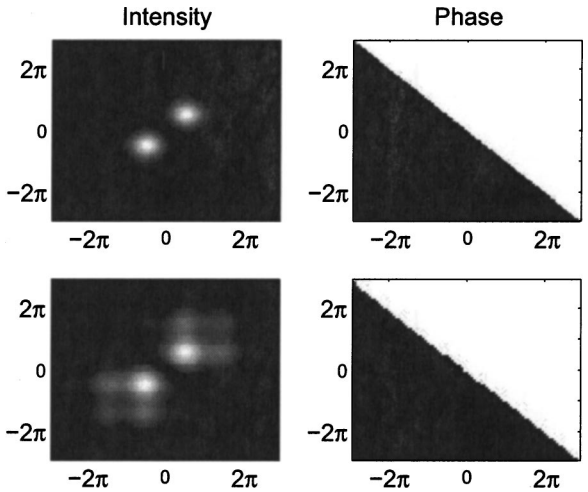

Fig. 5. Intensity (left) and phase (right) profiles of dipole solitons at $\mu = 1$ (top row) and $\mu = 1.70$ (bottom row) with $\nu_0 = 2$.

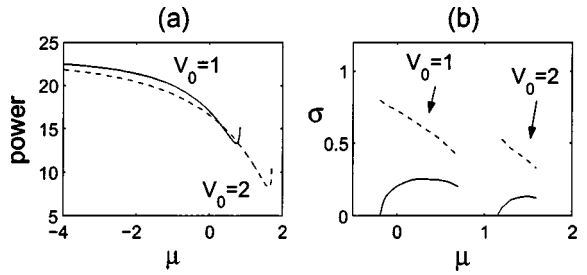

Fig. 6. (a) Normalized power P of dipole solitons versus μ for $\nu_0 = 1$ and $\nu_0 = 2$; (b) unstable eigenvalues σ of dipole solitons with $\nu_0 = 1$ and $\nu_0 = 2$; Re(σ), solid curve; Im(σ), dashed curve.

damental solitons of opposite phase (which is true especially in the strong-localization regime).

In Fig. 6(a), we see that at each potential value $\mathcal{V}_0$, the power of dipole solitons also has a minimum close to the upper bound μ_{dipole}. The VK stability criterion suggests that dipole solitons on the right-hand side of that power minimum would also be linearly unstable because of the existence of a purely real linear eigenvalue, just like fundamental solitons. Numerically, we have found this to be exactly the case. At $\mathcal{V}_0 = 2$, this minimum power occurs at $\mu \approx 1.64$, and the dipole soliton is VK unstable when $\mu > 1.64$; at $\mathcal{V}_0 = 1$, this minimum power occurs at $\mu \approx 0.74$.

The VK instability is not the only one encountered by dipole solitons. By simulating the linearized equations around dipole solitons, we have found another oscillatory instability lying on the left-hand side of the power-minimum point. This oscillatory instability is characterized by the presence of an unstable complex eigenvalue σ, with Re(σ) being the growth rate. Figure 6(b) shows the dependence of σ on the propagation-constant μ at two potential strengths, $\mathcal{V}_0 = 1$ and $\mathcal{V}_0 = 2$. We see that this oscillatory instability occurs in a limited μ interval, but this interval is much wider than that of the VK instability. Hence, this oscillatory instability is a more serious problem for dipole solitons. However, this instability can be strongly suppressed by higher potential strengths. As we can see in Fig. 6(b), the oscillatory instability at $\mathcal{V}_0 = 2$ is much weaker, and it occurs over a much narrower μ interval than that at $\mathcal{V}_0 = 1$. Thus, increasing the potential strength strongly stabilizes dipole solitons.

What is the effect of the oscillatory instability on the dynamics of dipole solitons? To answer this question, we pick the potential depth $\mathcal{V}_0 = 2$ and propagation constant $\mu = 1.3$. This μ value lies on the left of the power-minimum point (see Fig. 6a), hence the VK instability is absent. However, the oscillatory instability is present, as one can see from Fig. 6(b). We perturb this dipole soliton as in Eq. (26), except that now $u(X, Y)$ is a dipole soliton and $\hat{r}$ and $\hat{\theta}$ are the distance and angle of the point (X, Y) relative to the dipole center (0, 0). With $\epsilon = 0.01$ in the perturbation [Eq. (26)], the nonlinear evolution of the perturbed dipole state is shown in Fig. 7. We see that the oscillatory instability leads to the destruction of the dipole soliton: One hump of the dipole is eliminated, while the other survives. Thus, this unstable dipole evolves into a fundamental soliton accompanied by energy radiation.

Another important question is the robustness of a linearly stable dipole soliton and its ability to resist collapse. To address these issues, we have conducted a number of simulations for various $\mathcal{V}_0$, μ, and ϵ values. We found that under weak perturbations [$\epsilon \ll 1$ in Eq. (26)], the two humps of the dipole soliton could periodically exchange a small portion of energy and engage in an oscillatory motion. In other words, the dipole soliton remains stable. But when the perturbation is stronger, the dipole soliton can break its symmetry and evolve into a structure consisting of two unequal humps coexisting and mildly oscillating side by side. Sometimes, the dipole soliton can also lose one hump and evolve into a fundamental soliton plus radiation, similar to what happened in Fig. 7. For illustration purposes, we select $\mathcal{V}_0 = 2$ and $\mu = 1$, the same parameters as used for Fig. 4. When $\epsilon = 0.05$ which is relatively small, evolution of the perturbed dipole soliton is shown in Fig. 8. We see that the amplitudes of the two main humps in the dipole soliton oscillate alternately, but this oscillation is mild, and it does not break up the soliton itself. In addition, the phase difference between the two humps remains around the initial value of $-\pi$. However, when $\epsilon = 0.1$ which is a little larger, the evolution as displayed in Fig. 9 is different: There is a permanent transfer of energy from one hump of the dipole to the other, so that the original symmetry of the dipole soliton is broken. The new structure, which consists of two unequal humps and may be called asymmetric dipoles, appears to be stable, and it can sustain itself with mild oscillations for a long distance. The phase difference between the two humps in this new state, however, keeps increasing in a quasi-linear fashion (see Fig. 9). In other words, the phase relation of the original dipole soliton is broken.

Based on these simulations, we can conclude that linearly stable dipole solitons are also nonlinearly stable, but they are not as robust as fundamental solitons. Under moderate perturbations, they could break up and evolve into different states.

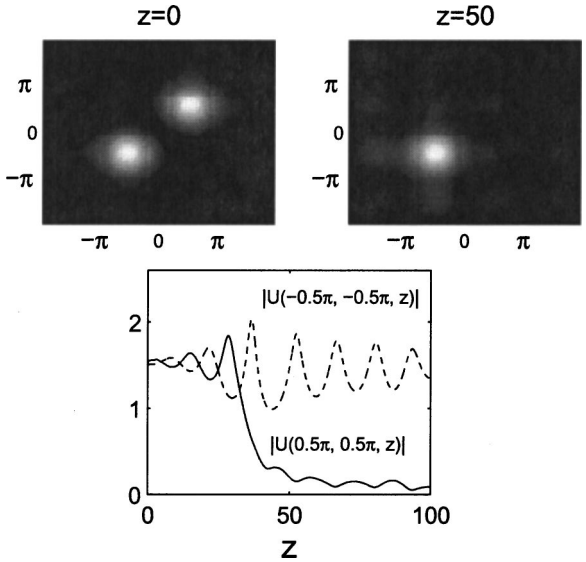

Fig. 7. Breakup of a linearly unstable dipole soliton into a fundamental soliton under weak perturbations. Here the dipole soliton has $\nu_0 = 2$, $\mu = 1.3$, and the perturbation [Eq. (26)] has $\epsilon = 0.01$.

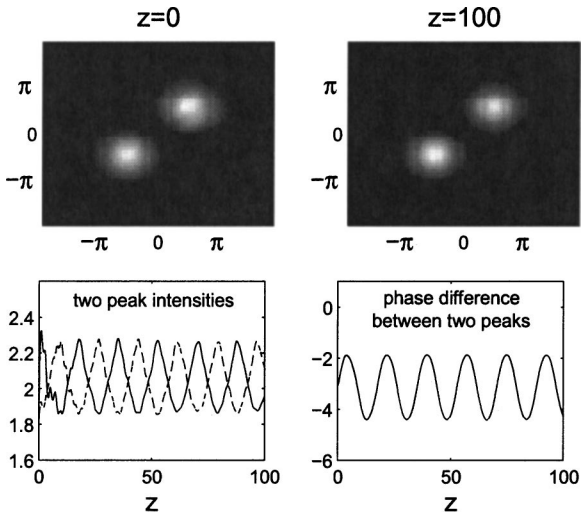

Fig. 8. Stable evolution of a linearly stable dipole soliton under weak perturbations. Here the dipole soliton has $\nu_0 = 2$, $\mu = 1$, and the perturbation [Eq. (26)] has $\epsilon = 0.05$.

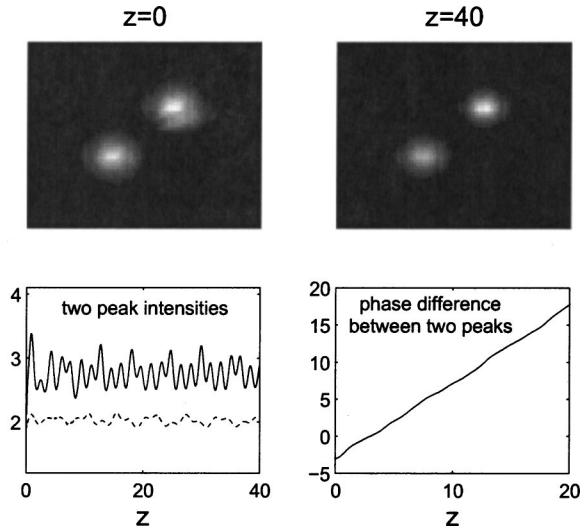

Fig. 9. Symmetry breaking of a linearly stable dipole soliton under stronger perturbations. Here the dipole soliton is the same as in Fig. 8 (i.e., with $\nu_0 = 2$, $\mu = 1$), but $\epsilon = 0.1$ in the perturbation [Eq. (26)] now.

6. VORTEX LATTICE SOLITONS AND THEIR STABILITY

Vector vortex solitons in a saturable nonlinear medium have been investigated extensively in the literature.[25–28] If both components are vortex modes, such solitons are always unstable, and they disintegrate into several filaments.[27] However, if one component is a fundamental mode while the other is a vortex (i.e., a fundamental mode guiding a vortex), such vortex solitons can be stable when the vortex component is weak.[26]

Vortices can also exist in a 2D lattice potential.[13,29] The structure and stability properties of lattice vortices differ drastically from their homogeneous-bulk counterpart.[25–27] The main difference is, that while conventional vortices have a ring shape (for which the intensity is angle independent), the vortex in a 2D lattice comprises four main humps superimposed in a square configuration with a phase structure that is topologically equivalent to the phase of a conventional bulk vortex. These vortex solitons, first reported in Ref. 13, are displayed in Fig. 10 for $\mathcal{V}_0 = 2$ and two μ values, $\mu = 1$ and 1.69. Note that at $\mathcal{V}_0 = 2$, the bandgap in Fig. 1 is $-\infty < \mu < \mu_{\max} = 1.7563$, while our numerics found these vortex solitons to exist in the interval $-\infty < \mu < \mu_{\text{vortex}} \approx 1.70$. We see that $\mu_{\text{vortex}} < \mu_{\max}$, thus vortex solitons do not exist in the entire bandgap of Fig. 1, similar to dipole solitons and unlike fundamental solitons. Again, the reason should be that these vortex solitons under the continuous-wave limit are not of separable type [Eq. (8)], while the bandgap of Fig. 1 was derived for separable wave functions. Indeed, these vortices always have zero intensity in the vortex center $X = Y = 0$, and nonzero intensity elsewhere. Under the continuous-wave limit, they can not be of separate type [Eq. (8)].

Next, we study the power diagram and stability properties of vortex solitons. The power diagrams at two potential strengths $\mathcal{V}_0 = 1$ and 2 are displayed in Fig. 11(a). These power curves are about four times higher than those of fundamental solitons, the reason being that a vortex soliton can be roughly thought of as a superposition of four fundamental modes under a vortex-phase structure. Note that these power diagrams also possess minimum points, these being at $\mu \approx 1.63$ for $\mathcal{V}_0 = 2$ and $\mu \approx 0.73$ for $\mathcal{V}_0 = 1$. This is similar to fundamental and dipole solitons, and is a sign that the VK instability would occur here (to the right-hand side of those power-

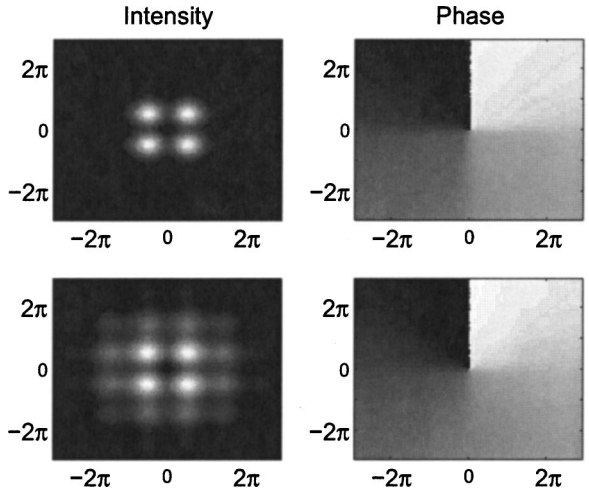

Fig. 10. Intensity (left) and phase (right) profiles of vortex solitons at $\mu = 1$ (top row) and $\mu = 1.69$ (bottom row) with $\nu_0 = 2$.

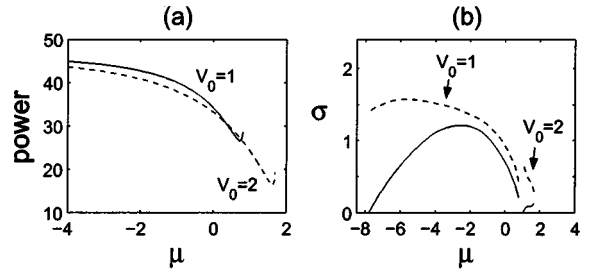

Fig. 11. (a) Normalized power P of vortex solitons versus μ for $\nu_0 = 1$ and $\nu_0 = 2$; (b) unstable eigenvalues σ of vortex solitons with $\nu_0 = 1$ and $\nu_0 = 2$; Re(σ), solid curve; Im(σ), dashed curve.

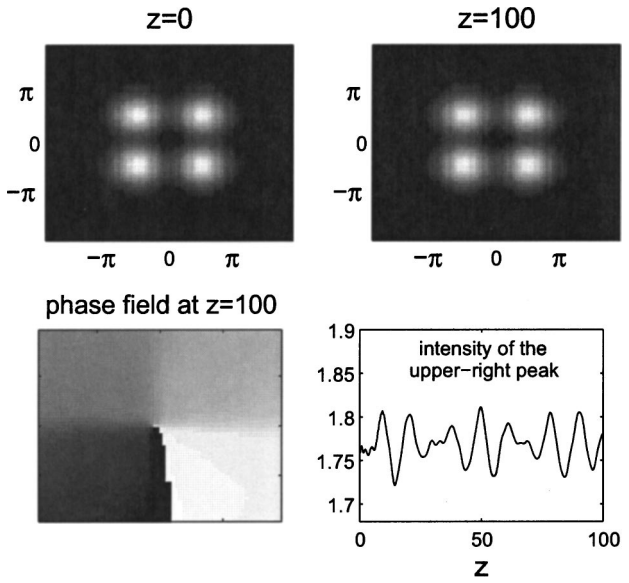

Fig. 12. Stable evolution of a linearly stable vortex soliton under weak perturbations. Here the vortex soliton has $\nu_0 = 2$, $\mu = 1$, and $\epsilon = 0.005$ in the perturbation [Eq. (26)]. The lower right figure shows the peak-intensity evolution of the first-quadrant hump of the vortex soliton. Intensity evolutions of the other three humps are similar.

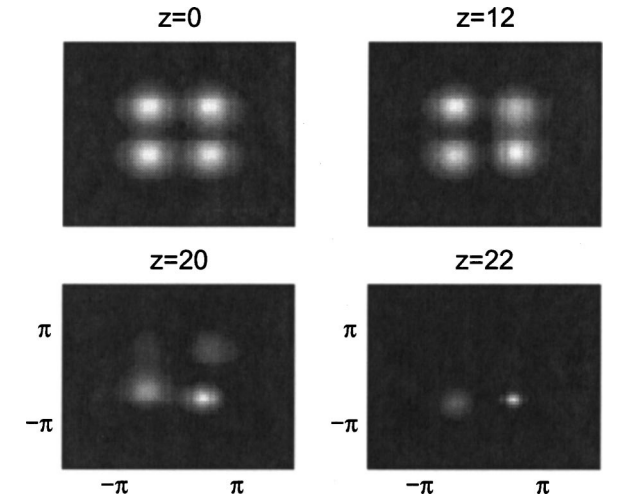

Fig. 13. Unstable evolution of a linearly stable vortex soliton under stronger perturbations. Here the vortex soliton is the same as in Fig. 12 (i.e., with $\nu_0 = 2$, $\mu = 1$), but $\epsilon = 0.02$ in the perturbation [Eq. (26)] now.

minimum points). But this VK instability is insignificant for vortex solitons because the interval of VK instability is very narrow [see Fig. 11(a)]. A more serious instability to vortex solitons is an oscillatory instability, just as for dipole solitons. The unstable eigenvalues σ versus μ at two potential strengths $\mathcal{V}_0 = 1$ and 2 are shown in Fig. 11(b). We see that this oscillatory instability is much stronger and broader than the VK instability, especially at low potential strengths. But it could be strongly suppressed by higher potentials. Indeed, at $\mathcal{V}_0 = 2$, this oscillatory instability is almost completely suppressed compared to the $\mathcal{V}_0 = 1$ case. Thus, as with dipole solitons, higher potential strength strongly stabilizes vortex solitons. We note that the present result of stable vortex solitons under high potentials is consistent with a similar result in the discrete 2D nonlinear Schrödinger equation when the intersite coupling is weak.[30] Indeed, if the potential is high, the intersite coupling in our vortex solitons is weak.

When vortex solitons suffer the oscillatory instability, it was shown in Ref. 13 that this instability triggers the breakup and local collapse of vortex solitons. What would happen if linearly stable vortex solitons were perturbed? Are they nonlinearly stable? How robust are they under strong perturbations?

To answer these questions, we again perturb vortex solitons in the form of Eq. (26), where $u(X, Y)$ is now a vortex soliton, and $\hat{r}$ and $\hat{\theta}$ are the distance and angle of the point (X, Y) relative to the vortex center $(0, 0)$. We have done a number of simulations for various $\mathcal{V}_0$, μ, and ϵ values. Our findings are that when a linearly stable vortex soliton is very weakly perturbed, it would remain nonlinearly stable. But if the perturbation is stronger, it would break up and locally collapse. For demonstration, we choose $\mathcal{V}_0 = 2$ and $\mu = 1$ as before. When $\epsilon = 0.005$ in Eq. (26), the simulation result is shown in Fig. 12. We see that this weakly perturbed vortex remains stable, and the amplitudes of its four main humps only oscillate mildly. In addition, the phase structure of the vortex is preserved throughout propagation. However, if ϵ is increased to 0.02, the vortex soliton disintegrates and collapses as seen in Fig. 13.

From the above numerical simulations, we see that even though linearly stable vortex solitons are also nonlinearly stable, they are less robust than dipole solitons (see Section 5), and much less robust than fundamental solitons (see Section 4). These results are consistent with those in a saturable nonlinear medium,[25,26] where it has been shown that vector fundamental and dipole solitons are always stable and very robust, while vector vortex solitons can be unstable and could disintegrate into dipole solitons.

7. CONCLUSION

In this paper, we have studied wave propagation in a two-dimensional photonic lattice. First, the bandgap structure for linear-wave propagation is determined. Then, inside the bandgap, various nonlinear localized structures in the form of fundamental, dipole, and vortex solitons are found, and their stability properties documented. When the propagation constant is not close to the band edge, solitons are strongly localized. In this regime, the fundamental solitons are always stable, while dipole and vortex solitons are stable only when the lattice potential is strong. It was also found that the fundamental solitons are the most robust as they can withstand strong perturbations without breakup. Dipole solitons are less robust, and vortex solitons are the least robust of the three. We have also shown that increasing the potential strength strongly stabilizes dipole and vortex solitons. When the propagation constant is close to the band edge, solitons spread to more lattice sites, and they are unstable because of the Vakhitov–Kolokolov instability.

ACKNOWLEDGMENTS

The work of J. Yang was supported in part by the National Science Foundation and NASA.

Corresponding author J. Yang's e-mail address is jyang @emba.uvm.edu.

REFERENCES

1. F. Lederer and Y. Silberberg, "Discrete solitons," Opt. Photon. News **13**, 48–53 (2002).
2. F. Lederer, S. Darmanyan, and A. Kobyakov, "Discrete solitons," in *Spatial Solitons*, S. Trillo and W. Torruellas, eds. (Springer, New York, 2001), p. 269.
3. D. N. Christodoulides and R. J. Joseph, "Discrete self-focusing in nonlinear arrays of coupled waveguides," Opt. Lett. **13**, 794–796 (1988).
4. A. B. Aceves, C. De Angelis, T. Peschel, R. Muschall, F. Lederer, S. Trillo, and S. Wabnitz, "Discrete self-trapping, soliton interactions, and beam steering in nonlinear waveguide arrays," Phys. Rev. E **53**, 1172–1189 (1996).
5. H. Eisenberg, Y. Silberberg, R. Morandotti, A. Boyd, and J. Aitchison, "Discrete spatial optical solitons in waveguide arrays," Phys. Rev. Lett. **81**, 3383–3386 (1998).
6. R. Morandotti, U. Peschel, J. Aitchison, H. Eisenberg, and Y. Silberberg, "Dynamics of discrete solitons in optical waveguide arrays," Phys. Rev. Lett. **83**, 2726–2729 (1999).
7. R. Morandotti, U. Peschel, J. Aitchison, H. Eisenberg, and Y. Silberberg, "Experimental observation of linear and nonlinear optical Bloch oscillation," Phys. Rev. Lett. **83**, 4756–4759 (1999).
8. T. Pertsch, P. Dannberg, W. Elflein, A. Bräuer, and F. Lederer, "Optical Bloch oscillations in temperature tuned waveguide arrays," Phys. Rev. Lett. **83**, 4752–4755 (1999).
9. G. Lenz, I. Talanina, and C. Martijn de Sterke, "Bloch oscillations in an array of curved optical waveguides," Phys. Rev. Lett. **83**, 963–966 (1999).
10. N. Efremidis, S. Sears, D. N. Christodoulides, J. Fleischer, and M. Segev, "Discrete solitons in photorefractive optically induced photonic lattices," Phys. Rev. E **66**, 046602 (2002).
11. J. Fleischer, T. Carmon, M. Segev, N. Efremidis, and D. N. Christodoulides, "Observation of discrete solitons in optically induced real time waveguide arrays," Phys. Rev. Lett. **90**, 023902 (2003).
12. J. Fleischer, M. Segev, N. Efremidis, and D. N. Christodoulides, "Observation of two-dimensional discrete solitons in optically induced nonlinear photonic lattices," Nature **422**, 147–150 (2003).
13. J. Yang and Z. H. Musslimani, "Fundamental and vortex solitons in a two-dimensional optical lattice," Opt. Lett. **28**, 2094–2096 (2003).
14. Z. Chen, H. Martin, E. D. Eugenieva, and D. N. Christodoulides, "Soliton-induced dislocations and discrete solitons in partially-coherent photonic lattices" (unpublished).
15. P. L. Kelley, "Self-focusing of optical beams," Phys. Rev. Lett. **15**, 1005–1008 (1965).
16. V. E. Zakharov, "Collapse of Langmuir waves," Sov. Phys. JETP **35**, 908 (1972).
17. R. Grimshaw, *Nonlinear Ordinary Differential Equations* (CRC Press, Boca Raton, Fla., 1993).
18. A. A. Sukhorukov and Yu. S. Kivshar, "Nonlinear localized waves in a periodic medium," Phys. Rev. Lett. **87**, 083901 (2001).
19. D. Mandelik, H. S. Eisenberg, Y. Silberberg, R. Morandotti, and J. S. Aitchison, "Band-gap structure of waveguide arrays and excitation of Floquet-Bloch solitons," Phys. Rev. Lett. **90**, 053902 (2003).
20. V. I. Petviashvili, Plasma Phys. **2**, 469 (1976).
21. N. G. Vakhitov and A. A. Kolokolov, Radiophys. Quantum Electron. **16**, 783 (1973).
22. L. P. Pitaevskii, "Dynamics of collapse of a confined Bose gas," Phys. Lett. A **221**, 14–18 (1996).
23. D. E. Pelinovsky, V. V. Afanasjev, and Yu. S. Kivshar, "Nonlinear theory of oscillating, decaying, and collapsing solitons in the generalized nonlinear Schrödinger equation," Phys. Rev. E **53**, 1940–1953 (1996).
24. T. Carmon, C. Anastassiou, S. Lan, D. Kip, Z. H. Musslimani, M. Segev, and D. N. Christodoulides, "Observation of two-dimensional multimode solitons," Opt. Lett. **25**, 1113–1115 (2000).
25. J. J. Garcia-Ripoll, V. M. Perez-Garcia, E. A. Ostrovskaya, and Y. S. Kivshar, "Dipole-mode vector solitons," Phys. Rev. Lett. **85**, 82–85 (2000).
26. J. Yang and D. E. Pelinovsky, "Stable vortex and dipole vector solitons in a saturable nonlinear medium," Phys. Rev. E **67**, 016608 (2003).
27. W. J. Firth and D. V. Skryabin, "Optical solitons carrying orbital angular momentum," Phys. Rev. Lett. **79**, 2450–2453 (1997).
28. Z. H. Musslimani, M. Segev, D. N. Christodoulides, and M. Soljacic, "Composite multihump vector solitons carrying topological charge," Phys. Rev. Lett. **84**, 1164–1167 (2000).
29. B. B. Baizakov, B. A. Malomed, and M. Salerno, "Multidimensional solitons in periodic potentials," Europhys. Lett. **63**, 642–648 (2003).
30. B. A. Malomed and P. G. Kevrekidis, "Discrete vortex solitons," Phys. Rev. E **64**, 026601 (2001).